Critical Review Vol. CR43, Optomechanical Design, ed. P.R. Yoder, Jr. (July 1992) Copyright SPIE

Optimization of the Optomechanical Interface Employing Diamond Machining in a Concurrent Engineering Environment

David J. Erickson, Roger A. Johnston and Anthony B. Hull
OCA Applied Optics, 7421 Orangewood Avenue
Garden Grove, CA 92641, USA
Telephone: 714/895-1667, FAX: 714/891-4356

ABSTRACT

Modern Single Point Diamond Turning (SPDT) technology offers new opportunities to address a large number of traditional problems in optical assembly and alignment. Traditional optical manufacturing rules-of-thumb have resulted from a lack of control over the Optomechanical Interface (OMI) . Because of the extreme accuracy associated with SPDT, conventional alignment methods can be replaced with deterministic and cost effective methods. These SPDT techniques have been demonstrated at OCA to be compatible with athermalization strategies, and with design-to-unit-production-cost (DTUPC) considerations.

1.0 INTRODUCTION

Over the past decade, the optical community has experienced an incredible growth in optical design capabilities. This has been driven in part by the increased pressure from more stringent system design requirements. It is also due in part to the ever-increasing power of computers and optical design codes. In an attempt to meet the often contradictory requirements of multi-spectral performance, severe light-weighting, athermalized operation, high-G environments and tight packaging constraints, the opto-mechanical designer has used every trick available. Armed with an optical design code and greatly enhanced CAD capabilities for mechanical layout, the designer has produced designs which employ multiple, general aspherics, often in non-axisymmetric configurations, with extremely tight fabrication and alignment tolerances.

This increase in both complexity and precision challenges the optical manufacturing community, even without considering the parallel pressures to reduce costs to minimum levels within very ambitious schedule constraints. Most of the challenges associated with converting these designs into functional hardware concern verification of the optical surface and control of the optomechanical interface.

2.0 THE OPTOMECHANICAL INTERFACE

The readers of this paper may have different perspectives on what are the crucial aspects of the optomechanical interface (OMI). Our perspective is that of an optical

engineering/manufacturing facility engaged in the specification, opto-mechanical design, fabrication and test of limited quantity, high performance, optical subassemblies and systems. This environment provides the most thorough interaction between the design and fabrication disciplines.

An optical designer working outside the manufacturing environment views the OMI primarily as a constraint defined by a standard list[1,2,3,4] of achievable manufacturing tolerances within which he must optimize his design. The mechanical engineer who packages the optical design creates the OMI as a means of locating and constraining elements within a tolerance band defined by the optical designer, while coupling the mechanical and thermal properties of the chosen optical materials to those of the system platform.

The mechanical engineer's understanding of the optical design may be only sufficient enough to translate the optical designer's prescription into element drawings. More thorough, usually, is his understanding of requirements relating to manufacturability. However, subtleties of the OMI as relates to higher precision levels may be missed.

The manufacturing engineer has broad knowledge of "real world" issues that relate to the OMI and views control of the OMI as one key to the successful assembly and alignment of the optical system. However, distance from the design process limits the extent that manufacturing factors influence design tradeoffs.

For moderate to low tolerance optical designs, these design functions can be successfully performed serially with limited interaction between disciplines. However, as design complexity and precision levels increase, close interaction between the design functions becomes more critical. At the extreme of complexity and precision, a concurrent engineering approach becomes essential.

We are addressing systems with aperture diameters on the order of 1 to 40 cm , and our discussion may not apply equally to larger or smaller systems. Table 2.1 represents the various precision regimes encountered in optical fabrication.[1,2,3,4] First, observe the precision levels that are produced in conventional optical fabrication. It can be seen that in the context of conventional optical fabrication methods, the OMI problem can be characterized by the need to control positioning of optical elements possessing relatively high surface accuracy with mechanical housings machined to one or two orders-of-magnitude lower precision. The housing machining is less accurate than the optical surfaces both because lesser precision is needed, and because lesser precision is available by conventional methods. If the interface could be produced to optical surface accuracy, errors associated with the interface would be negligible in most cases. However, conventional methods result in interfaces that usually have an influence on optical performance. This influence is a result of the imprecise methods used to produce the interfaces, and the assembler's inability to deal with multiple degrees of freedom in alignment. Thus, implementation of the interface is as stressing to optical performance as is implementation of the optical surfaces. We will consider interface factors in both conventional and diamond turning applications.

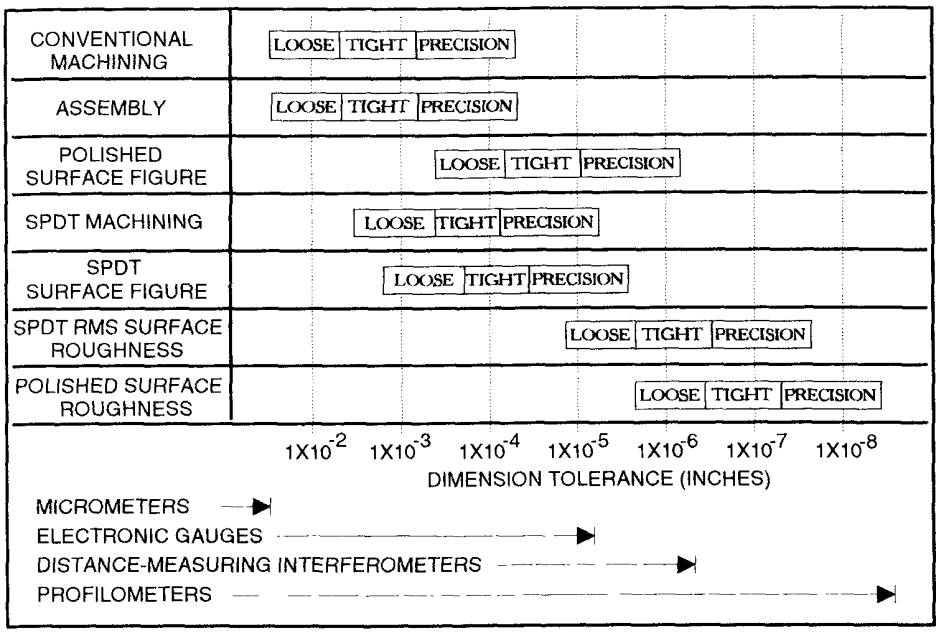

TABLE 2.1 : Precision regimes, comparing conventional machining and optical fabrication with Single Point Diamond Turning (SPDT).

3.0 CONVENTIONAL APPROACH TO INTERFACE CONTROL

Because of this disparity (See Table 2.1) between the high surface figure precision which can be achieved by conventional optical fabrication processes and the relatively poor dimensional control of interface surfaces, a number of techniques have been utilized to compensate for this deficiency. Among these are:

- mechanical indication of elements during assembly
- lapping and shimming for spacing control; "file-to-fit"
- monitoring of system aberrations or performance during element adjustment
- computer-aided alignment schemes
- lathe assembly
- matching of cells to glass after recomp for manufacturing actuals
- and mix-and-match techniques for large quantity applications.

As the precision and complexity levels increase, these approaches often become heroic in scope, usually becoming tooling and/or labor intensive.

3.1 Degrees of freedom

Even conventional approaches to simplify the OMI succeed because the design of mounting interfaces takes advantage of all available precision to minimize the number

of adjustments that must be made and verified by the assembler. A non-axisymmetric optical element can be misaligned with respect to any or all of its 6 degrees of freedom: 3 axes of translation and 3 rotations. Rotationally symmetric elements have 5 degrees of freedom. Fig. 3.1-1 defines the cartesian coordinate system that we will refer to in establishing the OMI, and in defining the errors in the interface. This discussion is limited to optical surfaces that are either figures of revolution, or are off-axis segments of figures of revolution. Although the techniques we are discussing are applicable to the relatively infrequent inclusion of anamorphic elements, to dispersive elements such as diffraction gratings and prisms, and to optics including discrete binary sub-components, we have chosen not to generalize discussion to include such optical surfaces. In this discussion, when 5 degrees-of-freedom are controlled, the interface is fully defined.

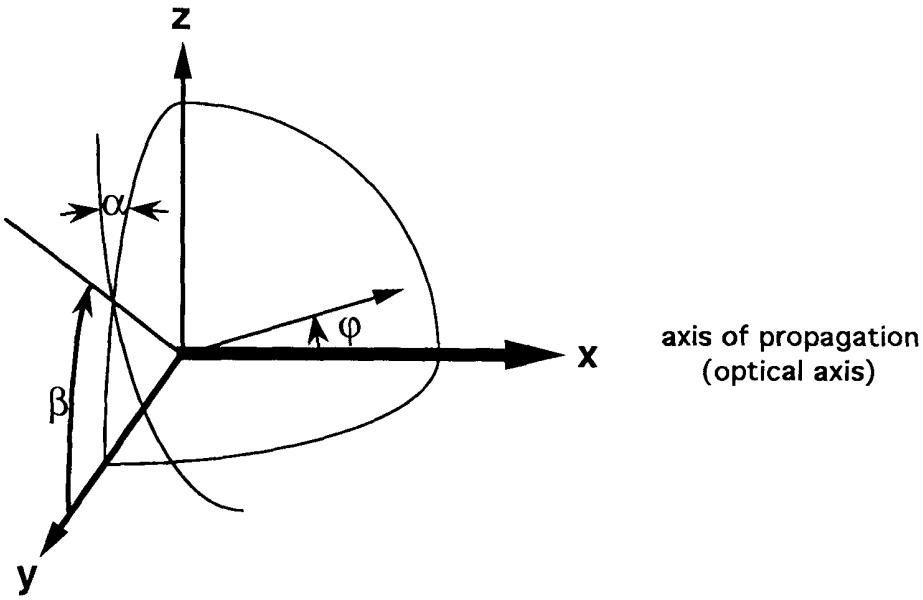

Figure 3.1-1 Cartesian Coordinate System. X defines the direction of propogation along the optical axis, and Y, Z define the perfect element rim plane. Any error in mounting an element into the perfect element rim plane will result in error in the surface normal ϕ as shown. The tilt will be angle α, and the axis of tilt is angle β. The six degrees of freedom that we discuss are the displacements x, y, and z, plus the angles α, β, and γ (not shown). γ is the degree of freedom corresponding to rotation about the x axis. We have limited this discussion to on-axis and off-axis figures of revolution.

Most conventional approaches of constraining the number of degrees-of-freedom are still left with 2 or 3, i.e. axial spacing and decentration. This is usually due to the shortcomings of conventional machining and/or glass shaping processes.

It would appear that without improving the precision of the OMI and optical element interface (C.T., O.D, Wedge, etc.), we are approaching the limits of system complexity and precision achievable through conventional manufacturing techniques.

4.0 THE SINGLE POINT DIAMOND TURNING MACHINE

4.1 Precision of SPDT Optical Surfaces and Interfaces

Table 2.1 demonstrates that with SPDT there is an immediate gain of at least an order of magnitude in the precision of mechanical features. Balancing this is some loss of optical surface figure and finish with respect to conventional polishing techniques. However, for infrared systems, this tradeoff can be quite acceptable. And by the appropriate choice of materials, figure and finish can be improved for visible applications by post-polishing. As we will see, the advantages gained by this improvement in mechanical feature precision are well worth these limitations.

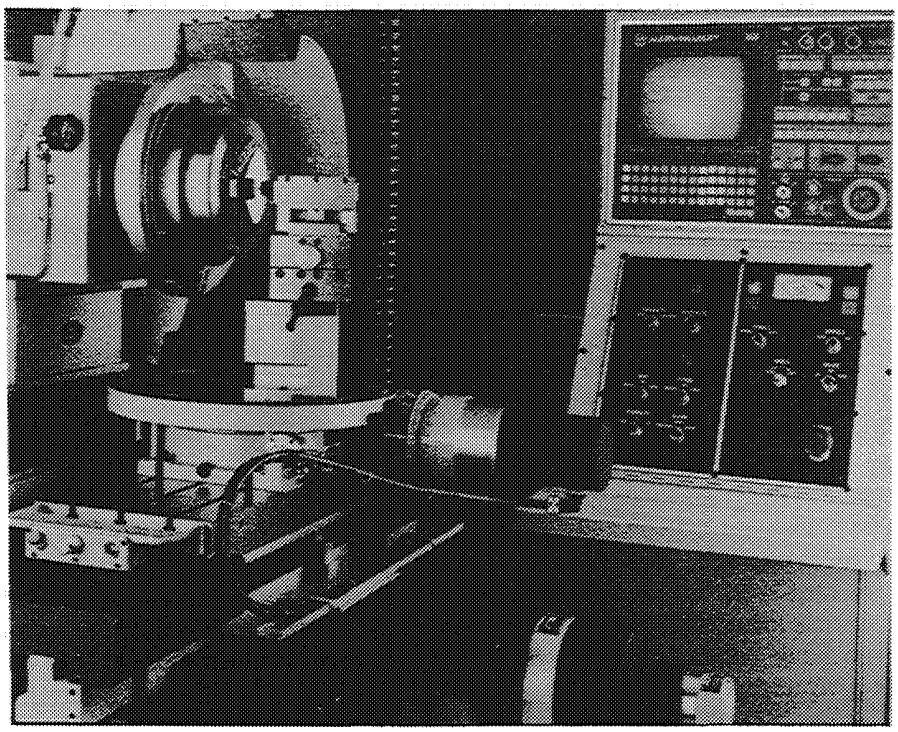

Fig. 4.1 Moore M-18 AG Single Point Diamond Turning Machine

4.2 Properties of the Single Point Diamond Turning Machine

The SPDT machine is a CNC lathe which obtains its great improvement in precision over conventional lathes through the enhancement of some of its features.[5] The spindle which holds the element to be turned has been replaced by an air-bearing or hydrostatic bearing because of its low friction properties and microinch runouts and stability. The cutting tool is now precision-lapped and of diamond for its hardness and heat transfer properties. The diamond tool is translated in two axes by a hydrostatic or precision roller bearing stage which exhibits very high straightness of travel. Whereas the conventional CNC lathe has an optical or mechanical encoder to transduce position, the SPDT machine utilizes a Distance Measuring Interferometer (DMI) accurate to microinch levels. The CNC controller has changed the least, except perhaps in the number of bits of accuracy encoded. In order to cut aspheric curves on complex hardware, the development of customized software is usually required to augment the functions provided by the controller. The SPDT machine is usually built over a massive frame (the OCA Moore M18 weighs approximately 4200 lbs) to minimize loss of precision due to flexure and vibration and thermal inertia. The room which houses the SPDT machine is optimally controlled for temperature, humidity and vibration, the result of which is a very critical long-term stability.

Table 4.1 lists some of the operating parameters of a typical SPDT machine (Moore M-18 Aspheric Generator). The OCA M-18 AG also utilizes a third rotary axis, on which the toolpost is mounted, which rotates under program control to always position the diamond normal to the curve being cut. This feature also allows easy access to the sides and backs of parts, facilitating single-set-up turning.

Spindle speed	0-2000 RPM
Spindle Axial Error	2 μin.
Tool Feedrate	0 - 4 in/min
Minimum programmable step	1 μin.
Z-axis travel	9 in.
X-axis travel	16 in.
Max. part dia.(over rotary table)	13 in.
Max part dia. (no rotary table)	22 in.
Max part dia. (with risers)	33 in.

Table 4.1 Moore M-18 AG SPDT machine operating parameters

The precision levels we are seeking fall within the parts-per-million CTE regime of most turnable materials, as well as a regime coinciding with strain magnitudes expected from mounting and centrifugal forces. In a well designed element, these may be the limiting factors to achieving total control over the OMI.

4.3 OMI control of element features with SPDT technology

The accuracy built into the SPDT machine suggests some obvious uses, such as producing optical curves, precision diameters, etc. However, of more importance to this discussion is how this capability can be used to configure the optomechanical interface to make assembly efforts more efficient and accurate. It is this exciting area of SPDT technology that allows one to turn modern optical designs into realizable hardware.

As described in Section 4, control of the OMI condenses down to eliminating degrees of freedom that need to be controlled at the assembly stage. There are very basic concepts that can be applied to designing elements for diamond turning that in many cases reduce assembly degrees of freedom to zero. These principles, single-setup turning, align-and-turn, and stack-and-turn, will be briefly described here and clarified through examples in Section 6.

4.3.1 Single Set-up Turning

The most basic concept of OMI control with SPDT hinges on the principle that any feature cut on a lathe in one set-up shares the same rotational axis. Add to this the microinch control of axial and lateral positioning inherent in SPDT machines and this principle expands to insure comparable accuracies on diameters and axial heights of faces.

4.3.2 Align-and-Turn

Not all elements can be created entirely in a Single Set-up configuration. In fact, it is often advantageous to have some surfaces already prepared by diamond flycutting or conventional polishing to provide references. By allowing for alignment of the element to the SPDT spindle face during its mounting, one is provided with a much larger range of possibilites for OMI control.

4.3.3 Stack-and-Turn

By combining the two principles above, and sequentially adding elements to the spindle without removing previously turned hardware, one can extend the inherent accuracies of the SPDT machine to whole assemblies. This represents the pinnacle of OMI control. By utilization of pinning or kinematic mounting techniques, assemblies can be turned, disassembled, conventionally worked (plated, post-polished, coated, painted, etc.) and reassembled without losing these micro-inch accuracies.

4.4 OMI control during system alignment

Many optical systems employ a hybrid mix of elements, some of which are appropriate for SPDT manufacturing techniques and others (beamsplitters, prisms, gratings, fold

mirrors, etc.) which still must be aligned to extremely tight tolerances. A class of optical elements for assembly which we call Metering Mirrors (see Section 5.7), are readily fabricated with SPDT techniques. These metering mirrors are designed to simulate the OMI of a previously diamond-turned element. The metering mirror may contain multiple reflective surfaces whose centers of curvature can represent various system datums (i.e., image plane location, element vertex or center of curvature location, or pupil locations). By locating these centers of curvature by interferometry or autocollimation, optical axes can be propagated through very complex folded paths. Section 6 includes more thorough descriptions of this powerful technique.

4.5 OMI and the optical test

By coupling the metering mirror concept with the well-known aspheric reflective null surface, the control of test conjugates for interferometric testing of aspheric elements or subassemblies is readily achieved.[6]

5.0 ILLUSTRATIVE EXAMPLES OF OMI CONTROL

5.1 Concurrent engineering: the cornerstone

So many of the examples to be given in the following section could not have been accomplished without the close interaction between the optical designer, the optomechanical designer, the manufacturing engineer, and the operators of the SPDT facility. The success of the approaches given hinged quite often on the understanding of the engineering team of specific SPDT machine capabilities and even idiosyncrasies. As system complexities increase and tolerances continue to tighten, the importance of more complete communication of machine capabilities will favor those endeavors which can control the whole design-through-fabrication cycle.

5.2 Designing for SPDT methods

The designer who can work with the technology of SPDT is far less constrained than the designer employing conventional technology. Sanger[5] has discussed many factors involved in producing SPDT optical surfaces. Clearly, unobscured mirrors and non-symmetric, irregularly-shaped and very fast aspheric optics can be efficiently produced with SPDT. For long-wave IR systems made from SPDT-compatible materials, there is no incentive to constrain the optical design to conics, nor is there a need to constrain the optical surface to be continuous. Similarly, unusual and efficient designs can be packaged by establishing the OMI with SPDT. Furthermore, the accuracy of this SPDT interface is so excellent that tolerances usually associated with alignment error may frequently be allocated to other system parameters. Although it is preferable that both the optic and the housing be produced by SPDT, we note that SPDT techniques used on a housing may interface efficiently with conventionally produced and lapped elements on optics, adjacent housings and optical benches.

SPDT methods are compatible with the most demanding spaceborne, military and scientific instruments. Examples below are representative of actual hardware produced at OCA incorporating SPDT to establish the OMI. Each example will show the application of a principle or principles discussed in Section 4.2. We start with a very simple (but significant) application of the principles, and in subsequent examples shall accumulate extensions to these principles, thus building to a description of implementation of a relatively complex system. The examples are also intended to be indicative of the range of application of the SPDT OMI methods, and suggestive of further extensions and developments.

5.3. Example 1: Fabrication and assembly of a 9-inch diameter germanium dome

Figs. 5.3-1, 5.3-2, and 5.3-3 show views of a germanium dome produced for a military application. The quarter-meter diameter, 6 mm thick germanium element extends beyond a hemisphere as a cylinder which serves as the mounting interface. The OMI is characterized by requirements for centrations of the germanium dome with respect to its titanium attachment ring reference surfaces to <0.001 in. both axially and laterally. These, as well as a <0.0003 in. germanium thickness uniformity requirement and wavefront requirement, are driven by optical performance considerations. The CTE values for the dome and ring materials were dissimilar enough to require 0.018 ±0.001 in. RTV thickness to control stresses over the operational thermal profiles. The titanium ring did not lend itself to being produced by SPDT methods; conventional lathe tolerances needed to be adequate. Developing production-level assembly techniques was a factor in the design effort.

It was realized that a variation of single-setup-turning could be developed to achieve all the dome requirements. We purchased the germanium generated to near-net-shape and went immediately to SPDT methods for curve generation. Fig. 5.3-1 shows the convex surface waxed to a turning fixture which is held on the SPDT faceplate by vacuum. This curve is cut from the cylindrical diameter to the vertex utilizing the 3-axis programming capabilities of the Moore M-18 AG. The convex surface serves as the reference surface for all future tooling. Optical performance is strongly influenced by the radius and figure control attained at this step.

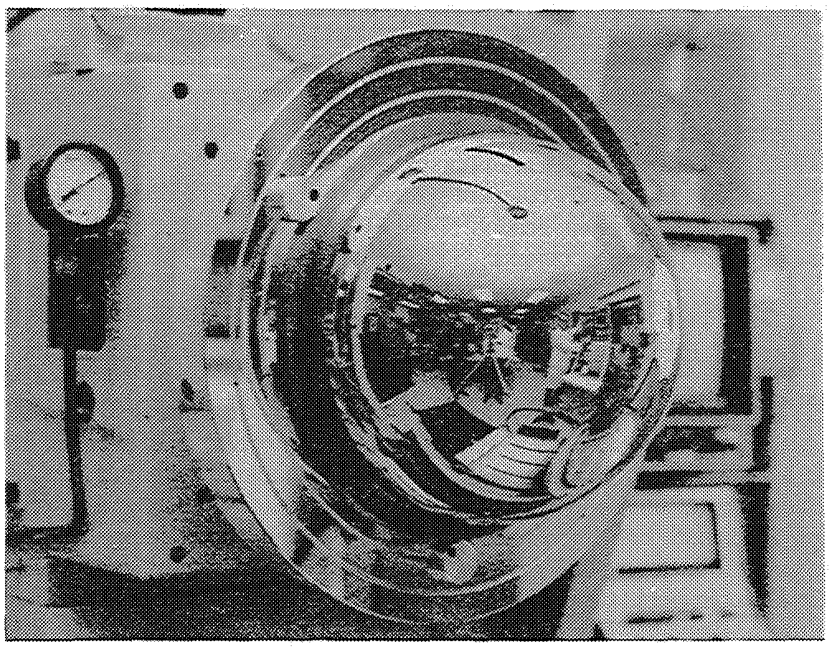

Figure 5.3-1 Generation of Convex Surface of Germanium Dome

The concave surface of the dome is produced by a variant of stack-and-turn where a vacuum chuck (similar to the assembly chuck shown in Fig. 5.3-2) is mounted on the SPDT machine and a spherical surface is turned on this chuck which matches the radius of the convex dome surface. Machine coordinates at this point uniquely define the center of curvature of both surfaces of the dome as well as the vacuum chuck. The dome is then merely installed into the chuck and the program run to cut the concave interior, the cylindrical inside diameter, the end face and the protective bevels. In a 50-unit production phase, this sequence was automated to a turn-key operation with a superb yield rate.

The same principles are applied to the assembly phase tooling. Fig. 5.3-2 shows a schematic of the assembly tooling. Again, SPDT machining was used to insure precision. The Spacing Tool was diamond turned at the chuck interface end to produce a face and outside diameter. The chuck was then turned in one setup to produce a concave surface matching the dome convex radius as well as a diameter and face to match the Spacing Tool features. Without removing the chuck from the SPDT spindle, the Spacing Tool was installed on the chuck and the length (minus allowance for graduated spacers) and outside diameter of the Alignment Mandrel interface surfaces were finalized. The outside diameter was matched to the Alignment Mandrel by trial during final cuts.

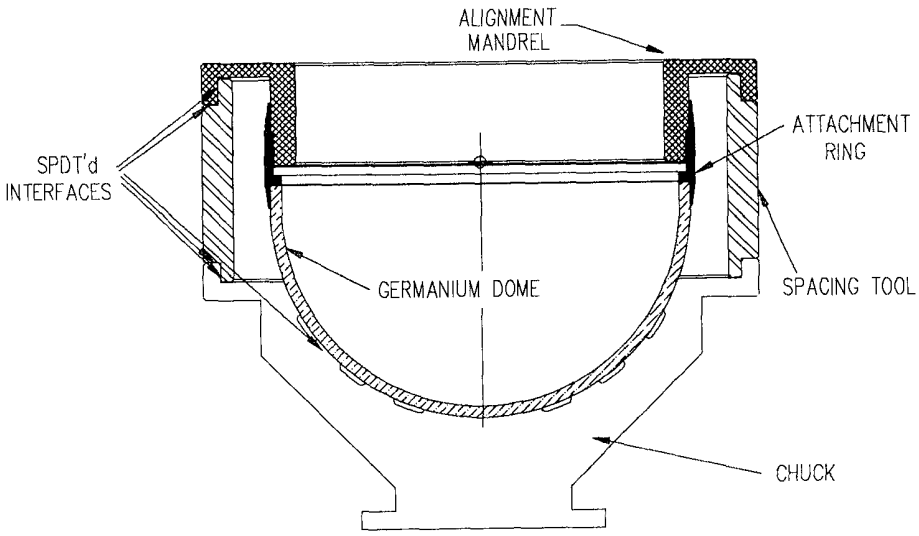

Figure 5.3-2 Germanium Dome Assembly Tooling

The final result was a dome assembly process which, after machinable spacer selection to compensate for Attachment Ring height variations, was essentially "drop-in" to <0.0007 in. TIR at a rate of one assembly per day. Fig. 5.3-3 shows a finished assembly mounted in test tooling.

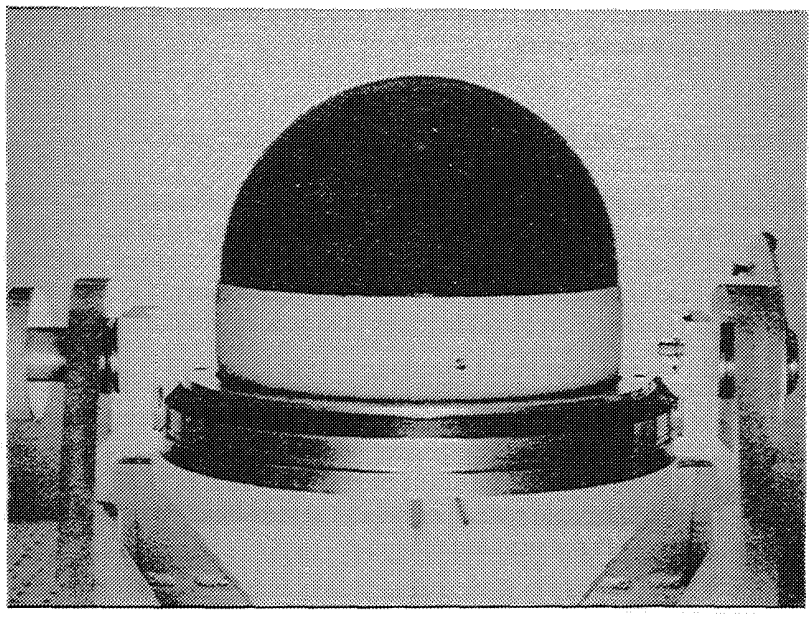

Figure 5.3-3. Germanium dome after final assembly

5.4. Single Point Machining of Metal Mirrors

5.4.1 Introductory comments

Aluminum mirrors, copper mirrors, beryllium, titanium and metal matrix composite mirrors clad with electroless nickel, and other material combinations can use some or all of the techniques that we shall describe below. It matters little if the optical surfaces are flat, spherical, or general aspherics with great departure from the nearest sphere. It also is only a small complication to mount off-axis segments of full mirrors. The underlying techniques are the same. We have selected several examples to illustrate specific OMI control methods we have found effective in mounting reflective elements.

Precision machining to establish the alignment is best done if the constraints of alignment are considered at the design stage. Alignment should constrain mirror fabrication on the SPDT machine. Should the optical sensor operate at either visible or short wave infrared wavelengths, the design should also consider the constraints of post polishing (nickel plating, polishing surrounds, etc.) Integral to the design of the optical assembly is the design of fixtures required for fabrication and alignment.

The viability of precision machining to establish the alignment requires that the design consider the pressures, centripetal forces, and stresses that both the mirror and the interface will experience during fabrication, and have a first resonant frequency higher than potential excitation frequencies found in fabrication. The single set-up turning of the optical interface is desired, but not always possible. Special cases include cutting off-axis mirrors, supporting thin mirrors on plates, and post polishing considerations. In all cases, the mounting conditions selected for fabrication processes will affect the performance of the mirror. The following are selected examples of optimizing the OMI in the production of metal optics.

5.4.2 Example 2: A Two Mirror Off-Axis Beam Expander

We selected this example (see Fig. 5.4.2-1) because it illustrates the fundamental technique of accurate transfer from the mirror-manufacturing interface to an assembly interface. The beam expander of this example employs two confocal parabolas and is required to operate in the visible and far infrared simultaneously. Because of its use in the visible, post polishing is required to remove the periodic residuals of SPDT.

The OMI is characterized by requirements for visible operation, fixed package size, $\lambda/12$ wave RMS (HeNe) collimation, and entrance and exit beam geometries. In addition, this off-axis afocal beam expander was designed to be low cost and direct replacement for several thousand existing systems. Our manufacturing methods needed to be tailored to accommodate production rates of several hundred units a month, a rate we could not satisfy with conventional techniques.

In its finished state the OMI of the primary mirror is a plane surface normal to the axis of the parabola and 0.10 in. below its vertex. This surface serves to reduce the possible

degrees of freedom of the primary to in-plane translations. This translation is further constrained by a pair of pins. The mirror is attached to the housing with six screws.

The OMI of the secondary mirror is a plane surface normal the the optical axis and 0.15 in. from its vertex. The motion of the secondary is constrained to translation along this surface. Oversized through-holes for the three screws that fasten the secondary, allow for small adjustments to system wavefront at final assembly.

The OMI of the housing consists of two SPDT parallel surfaces whose separation meters the assembly airspace. The OMI surface supporting the secondary serves the additional functions of boresight reference and next assembly interface.

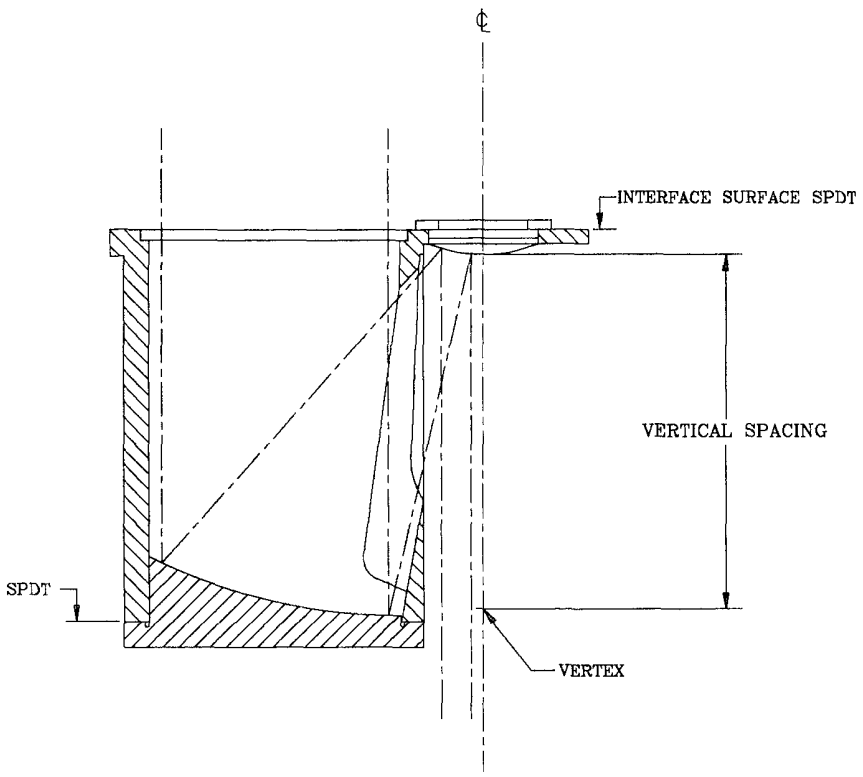

Figure 5.4.2-1 Two-mirror afocal telescope

5.4.2.1 Descripiton of SPDT process

The aluminium off-axis primary mirror was rough machined and stress relieved as were a surround and base plate. Although polishing single off-axis parabolic mirrors is within the capabilities of skilled opticians, it is more efficient to produce several in a multiple block and post-polish with a surround to fill in the spaces between mirrors. This efficiency is amplified when SPDT is used to generate the surface profile. The

three elements were assembled and the parabolic surface was final machined on a conventional CNC lathe. The primary and surround were then plated with electroless nickel to a thickness of approximately 0.005 in. Fig. 5.4.2-1 shows the primary mirror installed in its surround.

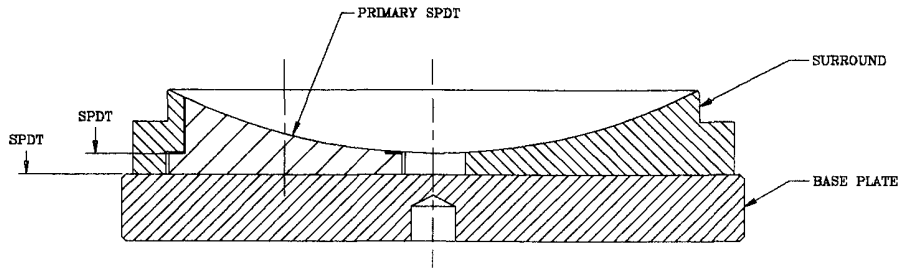

Figure 5.4.2-1 Primary mirror in polishing surround.

It is advisable to support the mirror during this manufacture with the same OMI used for assembly. Sometimes this desire cannot be realized and an additional OMI must be provided for manufacturing. Whereas the assembly OMI is the plane facing the secondary mirror, the preferred mounting surface for manufacture is the back plane of the primary. This requires a separate SPDT operation in which the back of the mirror is turned optically flat and parallel to the assembly OMI. It is appropriate to note here that these diamond turned reference surfaces can be used as alignment aids during in-process testing and are even more useful for interferometric monitoring of warpage during mounting operations.

The secondary mirror for this telescope, although used off-axis, was designed to be mechanically symmetric about its optical axis and oversized enough to serve as its own polishing surround. The OMI therefore could be turned in the same setup as the aspheric curve, thus allowing control of spacing and tilt of the optical axis.

After fine-tuning the process-dependent spacing parameters, assembly of these afocal telescopes consisted of monitoring of the flatness of exposed SPDT'd surfaces during torquing of the primary mirror screws and lateral adjustments of the secondary mirror to balance coma and boresight requirements. No shimming was required to achieve the $\lambda/12$ RMS (HeNe) collimation requirement.

5.5 Example 3: Fabrication and assembly of a monometallic cassegrain telescope

Figs. 5.5-1, 5.5-2, and 5.5-3 show a schematic and views of elements and the assembled cassegrain telescope for a spectrometer. The telescope has an 8-in. diameter primary mirror and is made entirely of 6061 aluminum to provide uniformity of thermal properties. The OMI is characterized primarily by a requirement that the alignment of the telescope remain stable throughout a temperature range from ambient to liquid

nitrogen temperatures. It was decided that utilizing precision machined interfaces would provide the most stable assembled structure. Other constraints included low cost, ease of assembly and alignment, and a desire to quantify relative motions of the individual mirrors and telescope stucture with respect to the focal plane. Fig. 5.5-1. shows a schematic of the mono-metallic telescope. The principal elements are the primary mirror, secondary support, secondary mirror, focus spacer, and retaining hardware. Fig. 5.5-2 shows these elements in exploded configuration after SPDT operations.

This telescope was designed with the intent of utilizing as many of the advantages of SPDT as possible. The primary and secondary were designed with integral reference spheres whose nominal optical centers of curvature coincided with the system focal plane. Several concurrent engineering design iterations were required to effectively incorporate these metrology features into the optomechanical design. The specific order of turning operations also affected the design. Incorporation of diameters and faces which could be utilized when flipping the mirrors for back side preparation was necessary. Finally it was felt that to achieve cryogenic performance, all surfaces should be subjected to the same machining operations.

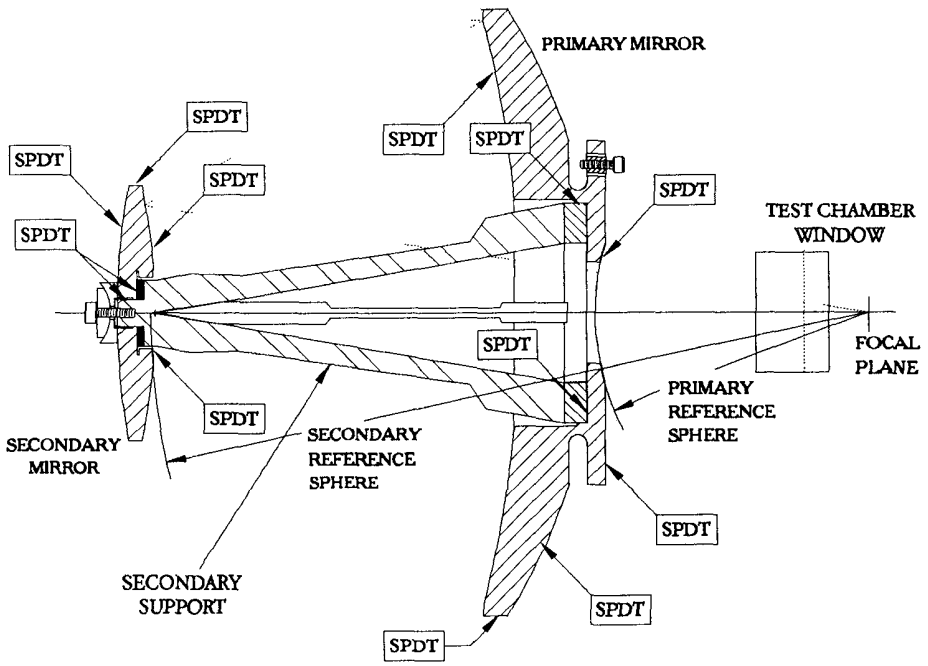

Figure 5.5-1. Schematic of SBIR mono-metallic telescope showing SPDT'd surfaces

After conventional machining operations to prepare the blank to a near net shape, the secondary mirror back surface was machined first. This established a precision mounting surface for the seocndary mirror aspheric turning operation. The secondary was then flipped and held to the SPDT spindle by vacuum. The outside diameter,

inside diameters, general aspheric optical curve, and the interface surface for the focus spacer were then turned, taking advantage of the accuracies afforded by the single-step-turning principle. See Fig. 5.5-1

The SPDT operations on the primary mirror also proceeded from its back. In one operation, the back mounting plane, the primary reference sphere, the spherical back of the primary mirror, and its outside diameter were turned. The part is then flipped and secured to the SPDT faceplate by its precision turned mounting plane. Axial locations of the front face with respect to back features are controlled by utilizing SPDT machine coordinates of the faceplate at the time of its last face-off. Lateral alignment of the primary mirror is assured by centering the primary to its outside diameter (align-and-turn) at which time the general aspheric primary mirror optical surfaces are cut. The interface plane for the secondary support is cut at the same time, at a precise distance from the prmary vertex. Finally the radially-defining diameter is cut to match-fit the conventionally-machined outside diameter of the secondary support base. (See Fig. 5.5-1)

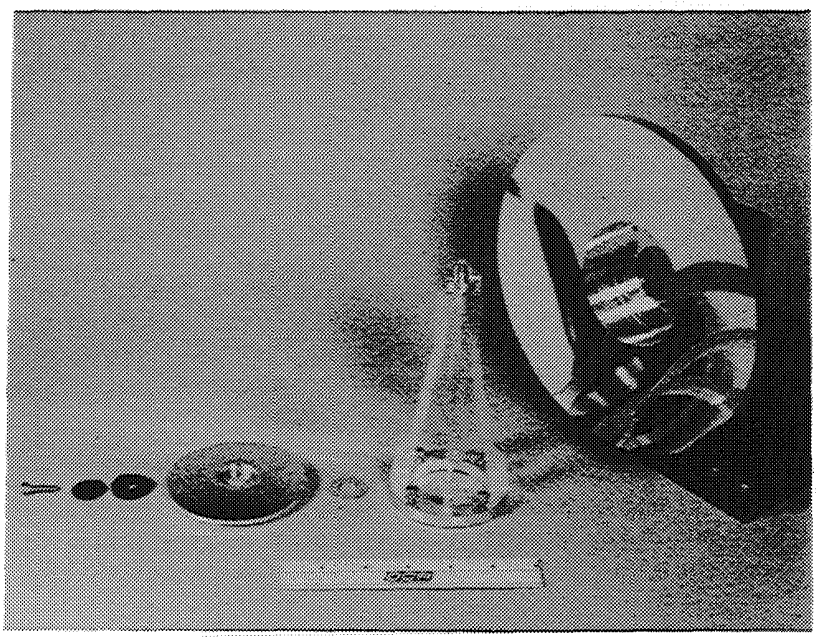

Figure 5.5-2. Exploded view of mono-metallic telescope elements

Without removing the primary mirror from the spindle, the secondary support was assembled to the primary with screws. The secondary mounting interface, a diameter and plane, are then turned on the end of the secondary support structure. Because of the accuracy of the stack and turn process, the optical axis of the primary is essentially transferred precisely to the mounting inside diameter of the secondary. After removal

of the primary from the spindle, the focus spacer is machined to nominal thickness and parallelism and the secondary mirror installed.

Fig. 5.5-3 shows the final assembly photograph of the mono-metallic telescope. Without any need for spacer thickness or wedge modification, this telescope could be disassembled and reassembled, and without any adjustments, produce a wavefront error of < $\lambda/4$ P-V (HeNe). Also fringes from the two metrology reference spheres can be observed at the same time.

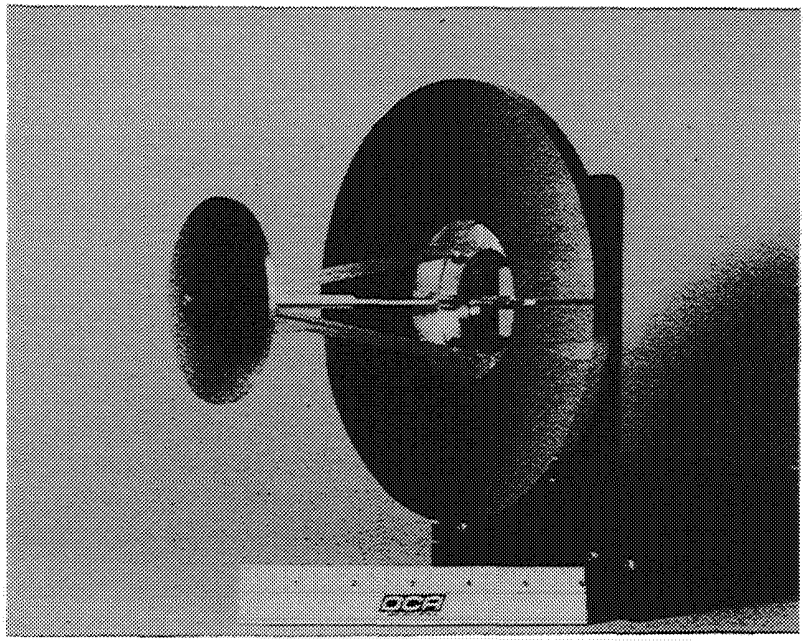

Figure 5.5-3. Assembled mono-metallic telescope

Thermal tests have not been run at this time, but assuming proper control of thermal gradients, this telescope should perform as designed or at least be easily monitored for element spacing and curvature changes.

5.6 Single point turning of refractive elements

5.6.1 Introductory comments

Although fabrication differences for refractive elements compared to reflective elements may be no more significant than modification of the cutting parameters to accommodate the ductility and other cutting properties of the material, mounting methods for refractive and reflective elements vary significantly. Schemes for mounting lens elements generally result in over-constraint and even the best schemes,

employing slotted and compliant retainers, distort elements. Also, adequate mounting methods for lenses may not be appropriate for mirrors.

One of the tasks facing the element fabricator is providing an OMI for subsequent assembly. For the simple case of a bi-convex lens, the OMI is composed of the optical surfaces and the rim of the lens. This rim defines the mechanical axis of the lens and may coincide with the optical axis if the latter was properly aligned during the edging operation[7] (See Fig. 5.6.1). For the condition where the mechanical and optical axis coincide within the allowed tolerances, the lens is "centered".

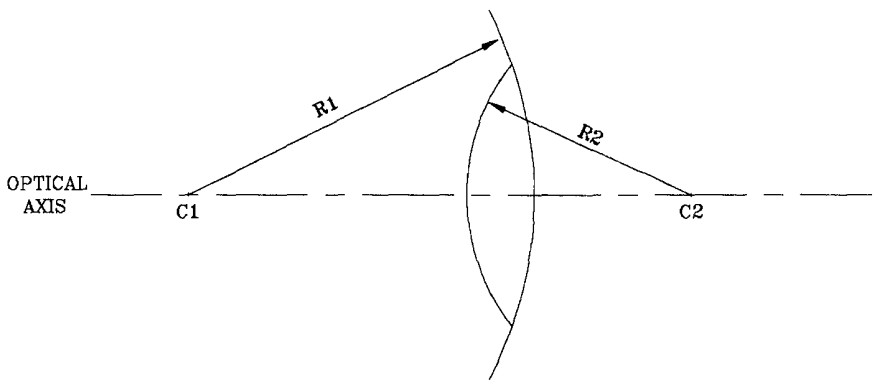

Figure 5.6.1. Condition for a perfectly centered element. The optical axis passes through both centers of curvature

Conventional lens manufacturing requires that polishing and edging operations be performed at separate times on different machines. The edging process requires the alignment of finished optical surfaces followed by grinding the rim. Today's optical designs demand precision, and are taxing the limits of conventional processes. Requirements for TIR <0.00005 in. are becoming common. Alignments to this precision level require great skill, are time consuming, and place delicate optical surfaces at risk of damage.

The separation of surface fabrication and edging is not necessary when SPDT methods can be employed. As illustrated in Table 2.1, SPDT enables direct machining to optical tolerances. The gap that existed between optical polishing and machining has been blurred, and the separate operations of surface finishing and OMI machining can now be accomplished on a single machine. The use of SPDT is limited somewhat by the selection of compatible materials. SPDT is ideally suited for infrared applications, where moderately loose figure requirements are complemented by moderately tight alignment requirements.

The infrared transmitting materials Ge, Si, ZnS, and ZnSe are readily turned using well established SPDT methods. Their turnability allows both the surface profile and OMI

to be produced in a single setup. In addition, the programming, and positional accuracy of SPDT machines makes it no more difficult to produce a general aspheric profile than a spherical profile. This in itself may result in major simplifications of the optical subsystem.

5.6.2. Example 4. Refractive element production by SPDT

As an illustration of single-setup SPDT, consider the volume production of a ZnSe apsheric element. Our discussion will begin with the conditions and tooling required for the alignment of an optical surface to a chuck. Here the process is common with both conventional edging and the SPDT. From this common point, the SPDT process departs with a discussion of the single point generating followed by optical surface fabrication. We will demonstrate, how in a single-setup , the aspheric surface, center thickness (C.T.), and diameter are machined.

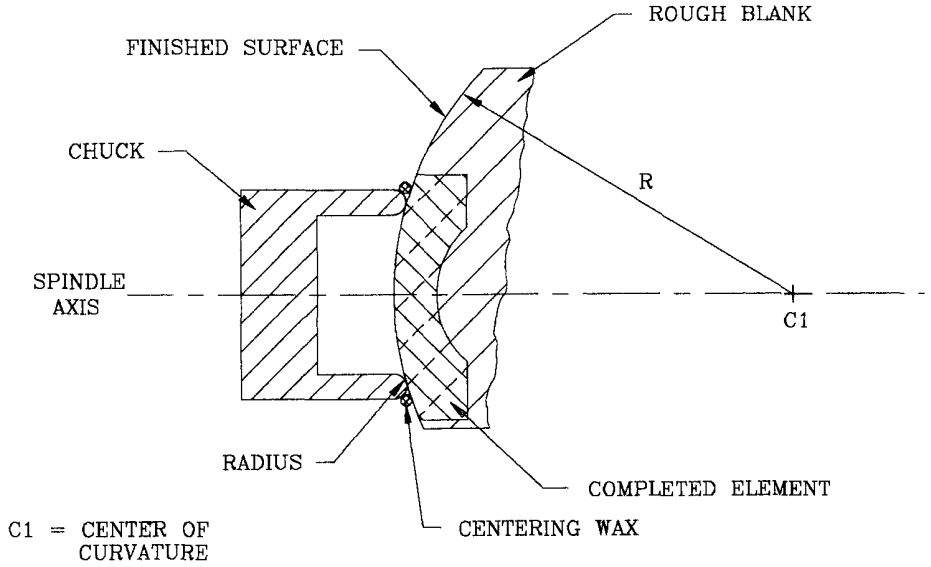

Figure 5.6.2-1. Element aligned for Single Point Generating

5.6.2.1 Element centering

Our process begins with a polished surface on an otherwise rough blank. As illustrated in Fig. 5.6.2-1, the polished surface of the element is placed firmly in contact with the radiused surface of the chuck and retained with centering wax. When this single spherical surface and chuck are in firm contact, motion is constrained to rotation about its center of curvature. Any decenter is accompanied by a compensating tilt, and centration is preserved. This greatly reduces the task of precision alignment. One need only assure the finished surface is in firm contact with the chuck and that sufficient material is available to yield a finished element. The TIR of this surface is monitored with an electronic gauge to accuracies of ±0.00005 in. while the element chuck ensemble is rotated on an air bearing. A process of heating, measurement, and

manipulating the lens is repeated until the desired TIR is achieved. In the case of precision lenses, TIR's < 0.00005 in. are not uncommon. Once cooled, a probe is inserted in the axial hole of the chuck, and contacts the vertex of the optical surface for measuring its location. This data is essential in calculating the position of the cutting tool in relation to the desired center thickness. The element is now in alignment with the chuck references and the task of precise transfer of this alignment from centering to generating to SPDT finishing is made easy.

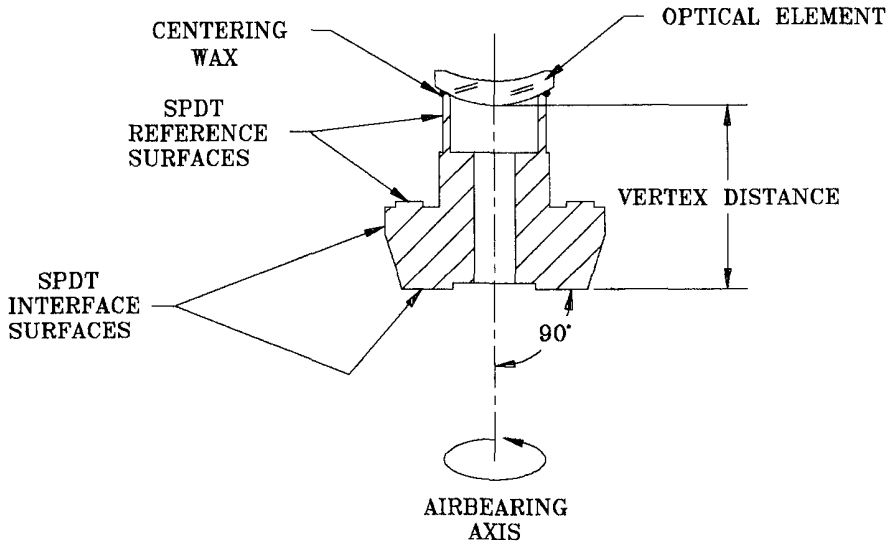

Figure 5.6.2-2 The transfer chuck provides single element alignment for many operations

5.6.2.2 SPDT chuck considerations

The quality of the element is dependent on the quality of the chuck, and therefore consideration must be given to the chuck's design and manufacture. Each chuck has built-in reference and alignment features to facilitate alignment prior to the centering and turning operations. Therefore, great care must be taken to assure these references are concentric to the chuck-radius supporting the element. One method of assuring this critical concentricity is to machine all surfaces in a single-setup.

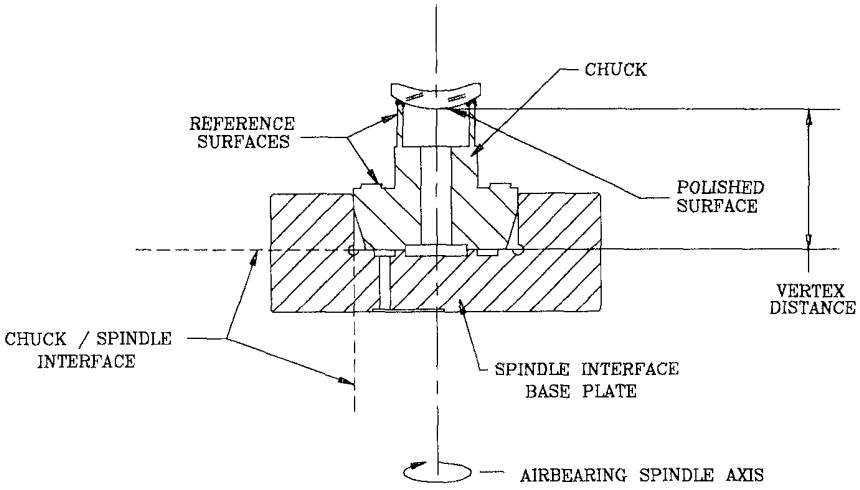

Figure 5.6.2-3. Chuck and airbearing spindle interface.

5.6.2.4 Single Point Generating (SPG) and SPDT finishing

With the chuck aligned to the spindle axis of a SPDT machine the process of generating can begin. Our element is an oversize rough blank. A single point tool consistent with high cutting rates is selected, and the programming of the SPDT machine is modified to allow for reciprocal operation. Modest cuts of 0.001 in. are advised while the surface is irregular to avoid knocking the element off of the chuck. As successive cuts remove these irregularities and the surface becomes more continuous, much larger cuts can be taken. We have removed as much as 0.010 in. in a single pass on ZnSe With the completion of the single point generating (SPG) operation the optical surface and OMI have been established. Sufficient thickness, usually <0.003 in., remains on the element for the SPDT finishing operation that follows. Starting with a single optical surface, an oversized blank, and the concept of single-setup turning precise alignment of the optical axis to the OMI is assured.

5.7 Example 5: Single Point Turning Of Lens Sub-cells And Drop In Assembly

5.7.1 Discussion of sub-cell concept

A natural extension of our single setup turning discussion above is its application to the manufacture of assemblies employing sub-cells. Sub-cells have been used for years in the production of precision optical systems, with many variations represented in the

literature.[7] The discussion of sub-cells that follows is intended to illustrate the application of single-setup SPDT.

Sub-cells are typically cylinders whose rim and faces serve as the OMI for an optical element. In applications where sub-cells are employed, one or more are assembled into a another cell or housing. From the perspective of parts count the sub-cell method appears to complicate the assembly. However if in a single setup all interface surfaces of the sub-cell are machined, one can readily achieve sub-micrometer control of the OMI. Another advantage of the sub-cell can be realized when an assembly requires multiple assembly-disassembly iterations for spacer trimming. If this disassembly is anticipated careful material selection is required to avoid galling, and within the limits of the environmental stress, the housing contact area should be minimized to facilitate smooth assembly. Additionally, the use of sub cells allows a modular approach to system manufacture, where sensitive elements are aligned and assembled as a module outside the system housing.

There are many schemes for retaining elements into these cells ranging from swaging to elastomeric suspension. Our discussion is limited to the latter. Here the skill of an assembler is applied to the alignment of the optical element onto a chuck rather than into a cell, and SPDT provides a precise OMI that facilitates drop in assembly. By mounting the element to a chuck as the first operation the assembler can verify the TIR of each optical surface and thus precisely control centering. The precision of this alignment is limited only by TIR gauging and operator patience.

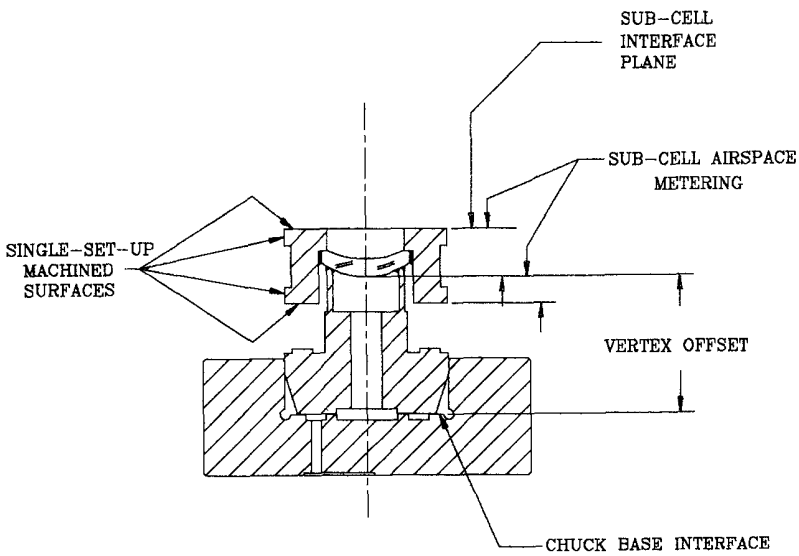

Figure 5.7.1-1 Oversize sub-cell ready for Single Point Machining

Once a lens is centered to the references of a chuck. An oversized sub-cell is bonded to the centered lens. (See Fig. 5.7.1-1) The lens, sub-cell, and chuck ensemble is set aside on a level surface while the adhesive cures. In most applications the sub-cell need only be aligned well enough to assure that OMI surfaces will clear during machining. In cases where the bond thickness uniformity is critical, and careful alignment is required, the sub-cell runout must be monitored during bonding.

With the sub-cell bonded to the element chuck ensemble, vertex offsets are measured. These offsets are used to establish the sub-cell airspace. (See Fig. 5.7.1-1) Machining of all interfaces is completed before removing the cell, lens, and chuck group from the SPDT spindle. Coolants used in SPDT will attack some adhesives and centering waxes and machining without coolant may be required.

In a single-setup, all interface surfaces of the sub-cell are SPDT'd and OMI accuracies of 1μm (4×10^{-5} in.) are readily achieved in production. Sub-cells of this precision allow drop in assembly. However, clearance between the sub-cell and housing must be provided, and this clearance is likely the single largest source of error. For assemblies under 3 in. in diameter, a clearance of 10μm (.0004 in.), is required for drop in assembly, worst case decenters resulting from this clearance are similar in magnitude.

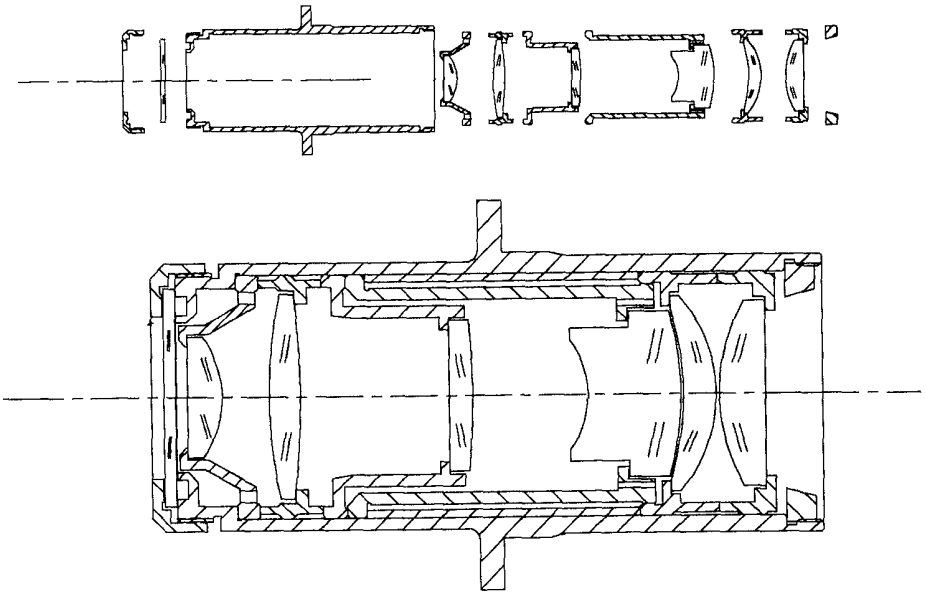

Figure 5.7.1-2 Schematic of a production drop-in assembly

Fig. 5.7.1-2 is a simplified sectional view of a production drop-in assembly. This low cost, controlled distortion, wide field lens was used for an infrared sensor. Its high performance required element wedge, tilt, and decenters of <10μm (<0.0004 in.). The image of several dozen completed systems were evaluated for rotational symmetry

and none departed by more than 3μm (0.00012 in.). In conventional manufacture, this dispersion would typically be on the order of 30μm and would have been unfavorable.

5.8 Example 5: Metering mirrors

5.8.1 Metering Mirrors: optical elements to assist assembly

Folded optical systems with high density packaging present the greatest alignment challenges. Such systems are becoming increasingly common as minimal volume and mass are needed to satisfy the operation of many developmental military platforms. Such optical packages must accomodate gyros, encoders, dewars, cables, sensors and analog logic, all related in a robust manner. One parameter used to describe such systems is packaging density; the volume of all elements plus optical paths divided by the package volume. Packaging densities in excess of 90% are often sought, and this density limits the ability to either provide internal alignment features, or to have access to alignment points. Fortunately, the method of metering mirrors mitigates this circumstance. Fig. 5.8.1-1 represents such an optical system.

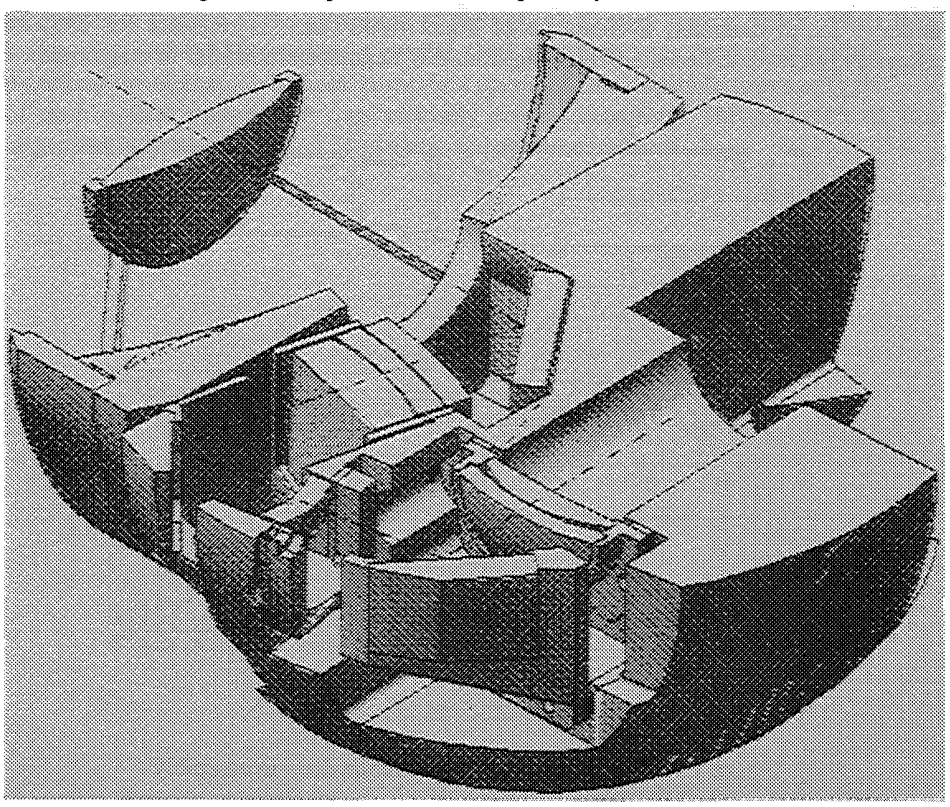

Figure 5.8.1-1 Representative Gimballed High Density Optical System

This system is packaged to a density of 93% with the aperture comprising 80% of the gimbal diameter, and the focal length comprising two times the gimbal diameter. Auxiliary methods are clearly necessary to establish the alignment of this system, and

the metering mirror method described in this section has proved to be a practical auxiliary method.

5.8.2 Metering Mirror Principles

Fig. 5.8.2-1 shows the centered mirror concept, and Fig. 5.8.2-2 shows a metering mirror of the sort that is used to build up optical elements to establish an optical system in the high density gimballed system in 5.8.1. Mirror centration here is similar to that described in Section 5.6 where we discussed the mounting of refractive elements. It is apparent that the metering mirror is perfectly centered with respect to the optical axis when two conditions are satisfied.

1. By geometrical identity, the optical axis must be perpendicular to the intersecting plane of the mirror's rim.
2. The center of curvature of the mirror lies on the system optical axis.

Condition 1 establishes the OMI plane tilt, and thus constrains two degrees of freedom. Condition 2 establishes the OMI cartesian coordinates (position in-plane and along the optical axis), and thus constrains three additional degrees of freedom. Since the mirror has rotational symmetry, the sixth degree of freedom is irrelevant, and the OMI is completely constrained.

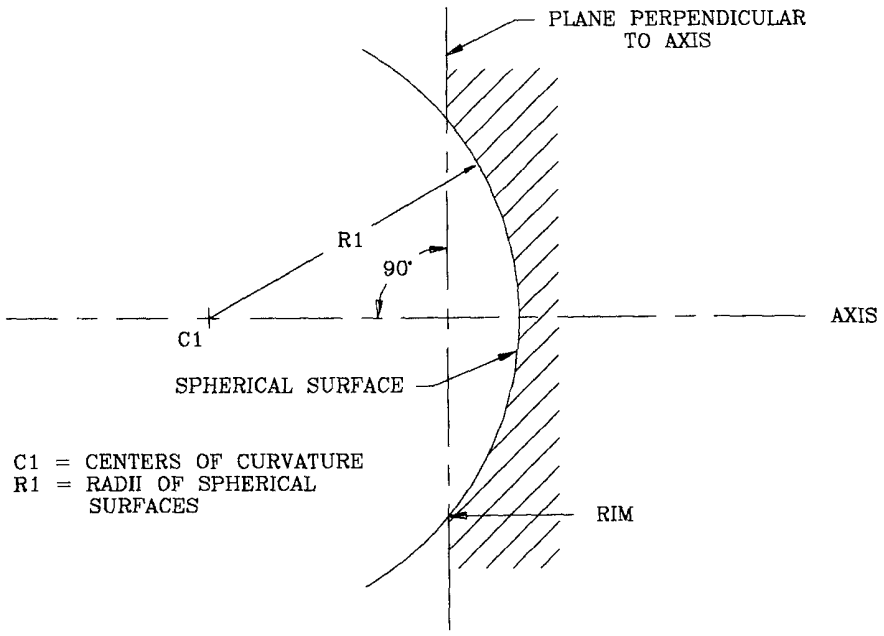

Fig. 5.8.2-1 Centered Mirror Concept

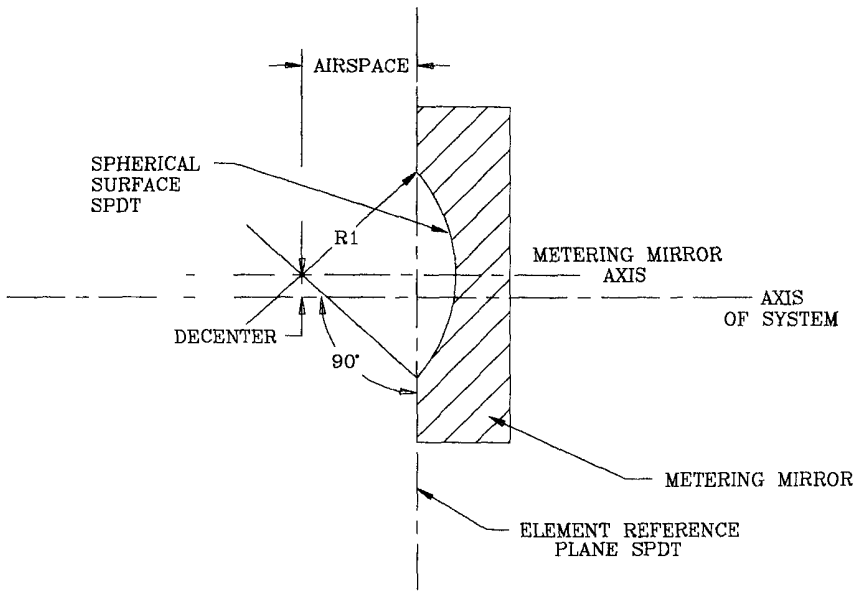

Fig. 5.8.2-2 metering mirror centration. The metering mirror is intentionally shown to be decentered from the system optical axis. Centration (translation) is sensed by interferometry, with central fringes resulting from decenter.

5.8.3 Use of metering mirrors to propagate the OMI

Metering mirrors are use to propagate OMI along the optical axis. To accomplish OMI propagation a fixed reference must be established against which all OMI are measured. A housing shoulder that precisely defines the optical axis serves this purpose and is used to support the reference interface plate. Refer to Fig. 5.8.3-1. Because it will not be removed until assembly is complete, attachment must provide rigid support without altering the reference surface figure.

The reference metering mirror is placed on the reference interface plate, which in turn is established at the primary datum of the optical housing. The reference metering mirror is not to be confused with the metering mirror. Note that the bore of the reference interface plate, and the diameter of the reference interface mirror are match machined by SPDT. Because the reference interface mirror will be taken in and out a number of times during alignment, the mirror surface S5 is relieved for minimal contact area to avoid binding during insertion. Binding could affect the registration or damage this critical interface.

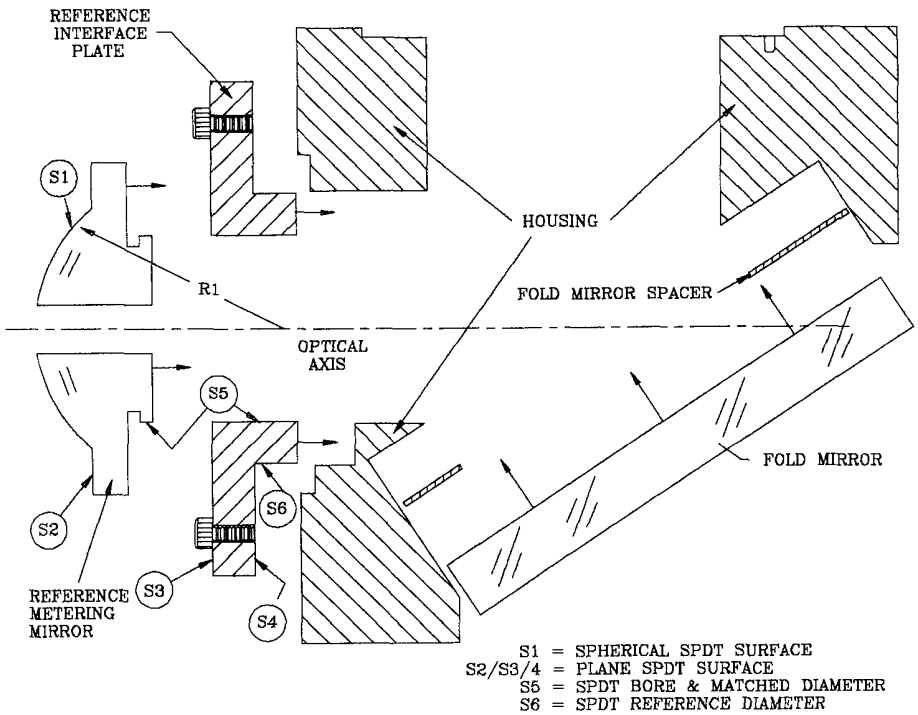

Fig. 5.8.3-1 Reference Metering Mirror and Reference Interface Plate. The optical axis is transferred precisely from the reference interface mirror at entrance of the housing to the reference metering mirror optical surface.

The metering mirror is quite straight forward to use. The assembler will need to have an interferometer of sufficient aperture to fill the full optical surface of the reference interface plate. Fig. 5.8.3-2 shows the set-up we use at OCA.

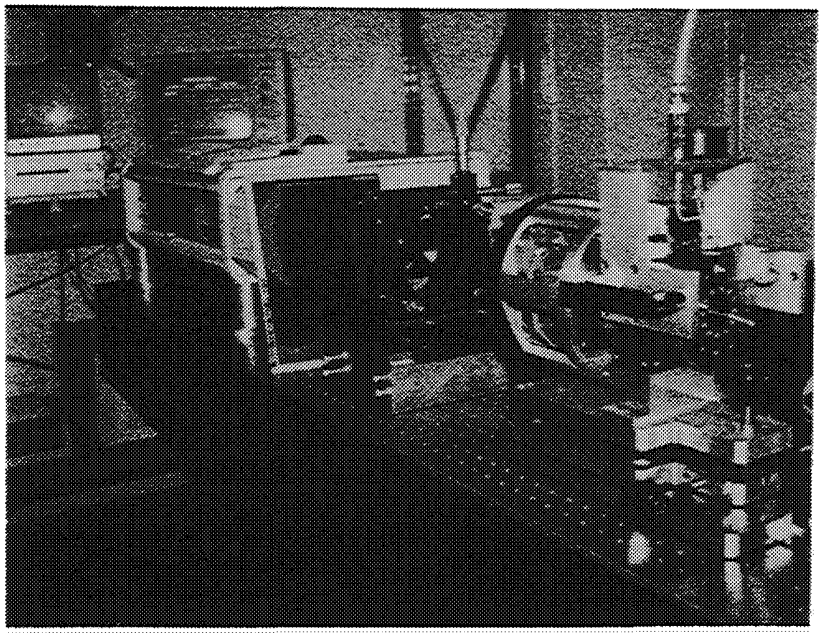

Fig. 5.8.3-2 Interferometric sensing of the metering mirror OMI transfer

It is of note that the accuracy of the method does not depend on the positioning of the interferometer in the set-up. The housing can be removed and replaced with no loss of accuracy. Two steps will establish the tilt, despace and decenter of the propogated OMI with respect to the datum. These two steps are as follows:

1. The reference metering mirror is removed as seen in Fig. 5.8.3-3. The tilt of the fold mirror is adjusted with respect to the metering mirror such that the plane wave front form the metering mirror is parallel to the plane wave front of the reference interface plate. This condition produces null fringes for each of these wavefronts. An example of the interferogram resulting form alignment is provided in Fig. 5.8.3-4.

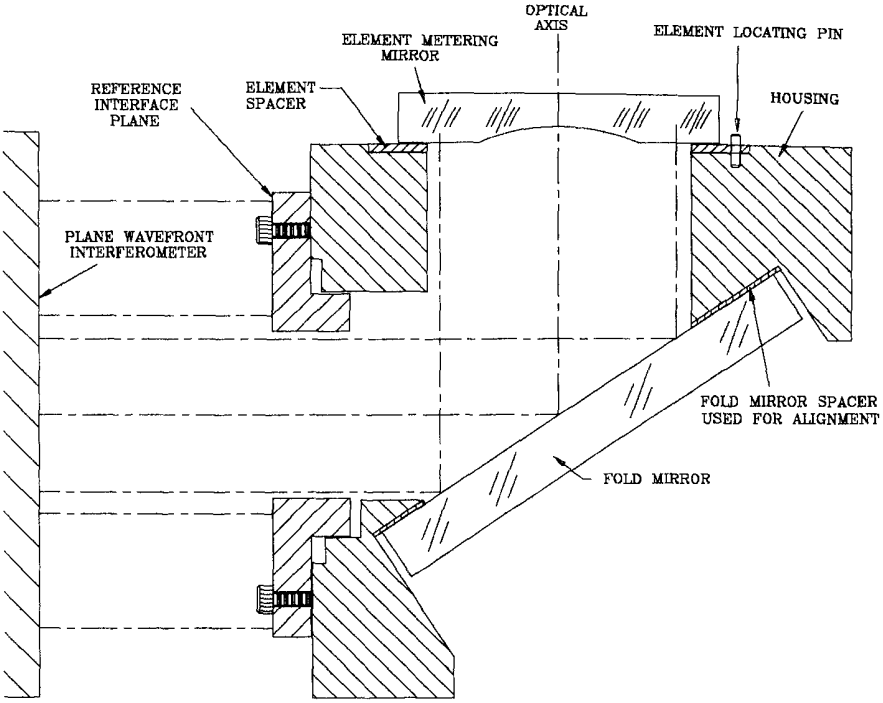

Fig. 5.8.3-3 Configuration for tilt adjustment. The reference metering mirror is removed.

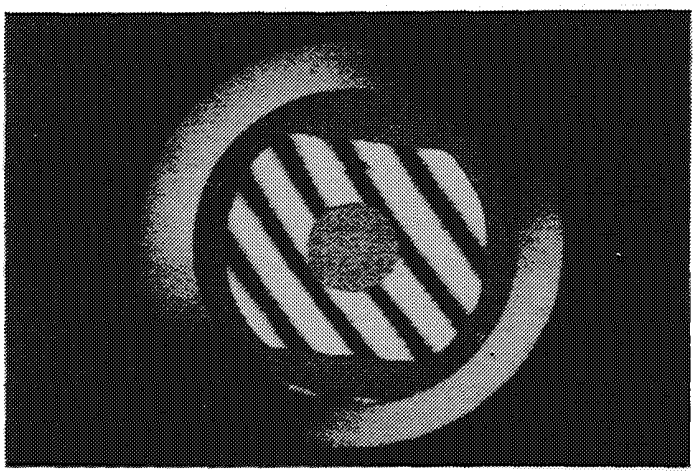

Fig. 5.8.3-4 Interferogram of adjustment for tilt. The difference between the two fringe patterns is 5 fringes (50 μin.) over a 3 in. diameter, which corresponds to a tilt of 21 μradians.

2. The reference metering mirror is inserted as seen in Fig. 5.8.3-5. The element metering mirror is adjusted until its center of curvature matches that of the reference metering mirror. This is termed the confocal position. This again will produce null fringes, however the null is with respect to the spherical surface of the reference metering mirror.

This two step process is repeated until the desired OMI alignment and despace is acheived for each element.

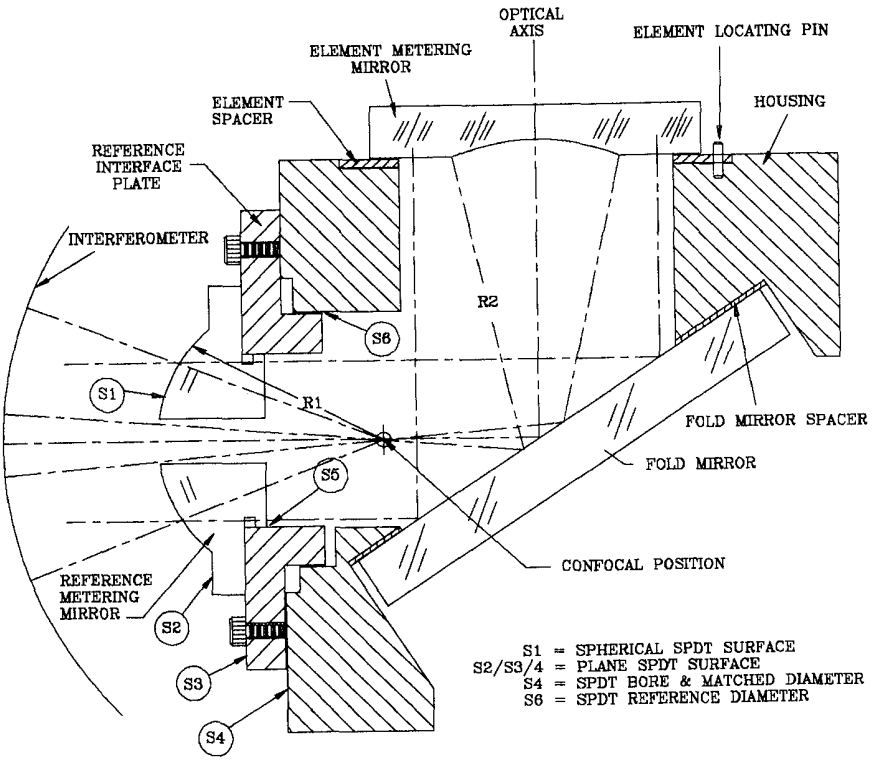

Figure 5.8.3-5 Configuration for despace and decenter adjustment. The reference metering mirror is installed.

5.8.4 Manufacture and validation of the metering mirror, and accuracy of the resulting OMI

The metering mirror, reference metering mirror, and reference interface plate are all produced as though they are optical elements. Carefully conditioned aluminum and SPDT single set-up techniques are used. Validation of the surface figure is easy to verify by interferometric testing.[6] A conventional interferometer set-up is used with a radius slide that includes a distance measuring interferometer.

Errors in using the metering mirror are dominated by interferometric determination of the optical axis and center of focus, and errors associated with the fabrication of the metering mirror are negligable with respect to this (typically 5μin. and 10 μradians).
Fig 5.8.4-1 expresses the relationship of errors in both despace and decenter to the F-number of the test. Here, λ is the wavelength in inches, the number of fringes is the difference between the fringe count for the reference metering mirror to that for the metering mirror. F/# is the F-number or radius of curvature of the metering mirror divided by the clear aperture of the metering mirror. Note that the radius of curvature is established by the distance of the OMI from the reference metering mirror. Note that, as the distance becomes long, the errors in spacing rapidly increase. The tilt is simply determined by the difference in number of fringes between the metering mirror and the reference interface plate, divided by the clear aperture.

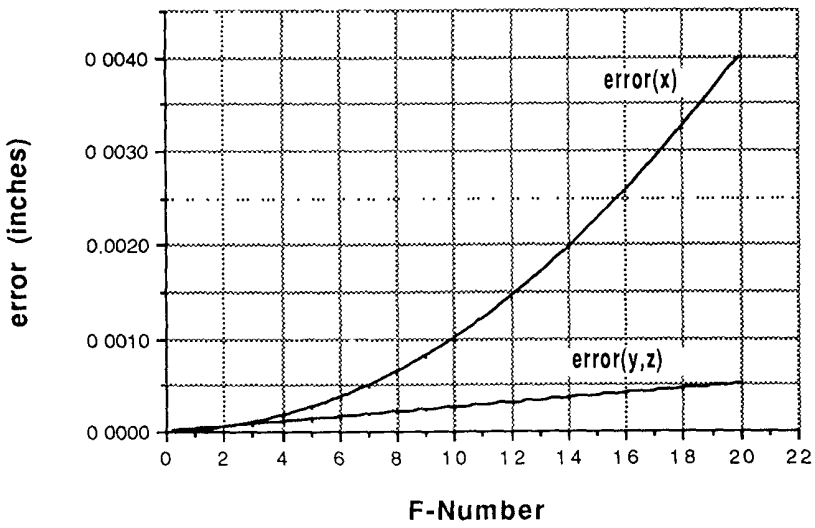

Figure 5.8.4-1 Errors associated with metering mirror alignments.

The despace error $\varepsilon_x = 4\lambda*(\text{estimated accuracy of number of fringes})*F/\#^2$ following Smith.[8] The decenter error $\varepsilon_{x,y} = \lambda*(\text{estimated accuracy of number of fringes})*F/\#$. The despace number of fringes is the difference in power derived from the interferogram of the reference metering mirror and the element metering mirror, each of which may be provided directly by the interferometric analysis software. The difference typically is accurate to better than ±0.1 fringe. The decenter error is set by the ability of the assembler to simultaneously null the fringes of both the reference metering mirror and the metering mirror, and we estimate this to be better than ±1 fringe

5.9 Assembly of the optical element in identity to the metering mirror position.

Once the assembler is satisfied that the metering mirror is located to the requisite accuracy, this positioning must be accurately transferred to the optical element. There are several ways of achieving this. For example, the metering mirror may simulate each degree-of-freedom of the OMI. The offsets that are used to establish (shim) the position of the metering mirror are used to establish the position of the component, and the component is bonded in place. The accuracy is mitigated by several factors:

- ability to maintain clean surfaces
- minimization of degradation of the shims
- ability to duplicate the loading forces experienced by the metering mirror
- different flexure properties between the element and the metering mirror
- nonuniformity and stresses caused by the curing of adhesives

Degradation in a carefully controlled environment typically is <0.0005 in.

If an interferometer with a precision slide is available, and the lens to be mounted has a spherical optical surface, greater precision can be acheived. In this case, the element cell will be SPDT finished to act as an auxillary metering mirror reference interface, and the reflection from the element will act as an auxilliary metering mirror sphere. The two step process described above (Section 5.8.3) is repeated but now with the auxillary metering. This usually does not obviate using a metering mirror at this location because the metering mirror is used to establish fold mirror positions prior to mounting any elements. The limiting factors will be only those described in Section 5.8.4, and the nonuniformity and stresses caused by the curing of adhesives mentioned above. Degradation in a carefully controlled environment typically is indistinguishable from that provided for despace and decenter in Figure 5.8.4-1, and for tilt as discussed in Section 5.8.4 (tilt is typically controlled to 10 to 30 μradians, which to date is seldom required).

6.0 FUTURE DIRECTIONS

We have considered the implementation of current SPDT technology to efficiently establish the OMI for complex systems. For many cases, the OMI can be established to between one and two orders-of-magnitude better than with non-SPDT techniques. In others, the interface can be so simplified that producibility is greatly enhanced. We expect that future designs will increasingly exploit this improvement jump in the following manners:

- Design of more complex and densely packaged systems
- Reallocation of the tolerances to acknowledge the OMI accuracy available
- Design for simplification of the interface, and production drop-in assembly

In order to affect this exploitation, there will be a closer fusion between the optical and mechanical designers and the manufacturing operation. Fortunately, this is increasingly being done in the current industry drive for concurrent engineering. Designers will

want to educate themselves on what can be accomplished, and not rely on old rules-of-thumb for assembly.

Simultaneously, capability to manufacture the OMI will be increasingly stressed. We are already seeing instances where designers are defining requirements for which the one-to-two order of magnitude improvement cited above is insufficient. Areas that may be productive in ameliorating these limitations over the next decades are apparent. As defined for this paper, we are primarily concerned with assemblies of characteristic dimensions of the order of 1 to 40 cm. Different factors would apply to either large assemblies, or to micro-miniature assemblies, and a list corresponding to divergent size regimes may be significantly different. Many of the potential developments we list in Table 6.0-1 will affect both the OMI and the optical surface.[9]

Table 6.0-1 Future directions to further improve manufacturing the omi

Better Position Controls:

- Improved position sensors, defining the relative location of the tool edge and work piece possibly including interferometric sensing of the diamond edge
- In-situ optical metrology (independent of the machine's metrology)
- Improved work piece mounting methods
- Stiffer machines
- Micro-damping through positional feedback
- Improved servo controls
- More adaptable control software and AI corrections from in-situ metrology
- More agile tool carriages
- Better environmental controls

Better understanding of materials and tools:

- Tribology of the tool, work piece interface, and elastic/plastic properties of micro-cuts
- Active temperature control (cooling or heating) of the tool
- Alloys with improved homogeneity, isotropy, hardness, grain structure and micromechanical properties (microyield, microcreep), and with minimum defects
- Improved tools
- Tools and methods to work strategic materials like beryllium, SiC and glass ceramics which are largely inaccessible for these techniques

Fusion with other techniques

- Laser milling
- Autonomous alignment verification methods using embedded binary optic and holographic elements

- Extension of these methods for establishing precision surfaces into ductile grinding techniques for materials not accessible to diamond tools.

7.0 CONCLUSION

The power of SPDT techniques to establish the OMI to an accuracy to one or two orders-of-magnitude better than that achieved by conventional alignment methods has been explored, and the practical manufacturing approach that OCA has been using has been described through a series of examples. The underlying principles of single set-up turning, align-and-turn, and stack-and-turn have been defined, and starting with the mounting of single refractive or reflective elements, we have systematically introduced concepts through examples. This has led to description of the more advanced metering mirror methods that are effective for a wide range of alignment problems including those associated with high density, folded systems including decentered off-axis aspheric elements. Such SPDT methods are available to new systems, and are being practiced in the optics manufacturing community with encouraging results. The authors have stressed the importance of concurrent engineering to achieve the potential precisions and efficiencies of these SPDT techniques to establish the OMI. Consideration is given to potential advances in techniques, materials and machines that may yield further precision and simplicity to establishing the OMI.

8.0 ACKNOWLEDGEMENTS

The authors wish to acknowledge our colleagues who have participated in establishing this technology at OCA, and have participated in discussions or provided comments relevant to this paper. Bert Fischer has helped develop these ideas, and has implemented them on the our SPDT machines. Ralph Scicchitano has assisted in preparing figures for this paper. Bill DeBoynton has challenged these OMI concepts with both increasingly stringent design demands, and with insights into what can be machined. Dan Barber has always been willing to woodshed new problems.

9. REFERENCES

1. R. H. Ginsberg, "Outline of Tolerancing (from Performance Specification to Toleranced Drawings)", Optical Engineering, Vol. 20(2), pp. 175-180, 1981.
2. P. Kuttner, "Trends and Limits in the Production of Optical Elements and Optical Systems", Advances in Optical Production Technology II, SPIE Procedings Vol. 163, pp. 24-30, 1979.
3. R. E. Parks, "Optical Component Specification", 1980 International Lens Design Conference, SPIE Procedings Vol. 237, pp. 455-463, 1980.
4. J. L. Plummer, "Tolerancing for Economies in Mass Production of Optics", Optical Systems and Components Specifications, SPIE Procedings Vol. 181, pp. 90-111, 1979.

5. Gregory M Sanger, "The Precision Machining of Optics", Applied Optics and Optical Engineering, R. R. Shannon and J. C. Wyant, Volume X, pp. 252-390, Academic Press, Inc, 1987.

6. D. Malacara, Optical Shop Testing,John Wiley and Sons, New York, 1978.

7. P. R. Yoder, Jr., Opto-Mechanical Systems Design, Chapter 4, Marcel Dekker, Inc, new York, 1986.

8. W. J. Smith, Modern Optical Engineering, The Design of Optical Systems, Second Edition, Chapter 11.2, McGraw Hill, Inc., New York, 1990.

9. D. L. Decker, "The Future in Diamond-Machined Optics", Ultraprecision machining and Automated Fabrication of Optics, SPIE Proceedings Vol. 676, pp. 2-7, 1986.